Evidence of a circularly polarized light mode along the optic axis in *c*-cut $NH_4H_2PO_4$, induced by circular differential reflection and anomalous birefringence

2010 J. Phys.: Condens. Matter 22 095902

(http://iopscience.iop.org/0953-8984/22/9/095902)

J. Phys.: Condens. Matter **22** (2010) 095902 (11pp) doi:10.1088/0953-8984/22/9/095902

Evidence of a circularly polarized light mode along the optic axis in *c*-cut $NH_4H_2PO_4$, induced by circular differential reflection and anomalous birefringence

Werner Kaminsky[1,4], Steven Steininger[1], Javier Herreros-Cedres[2] and Anthony Michael Glazer[3]

[1] Department of Chemistry, University of Washington, Seattle, WA 98195, USA
[2] Departmento de Fisica Basica, Facultad de Fisica, University De La Laguna, La Laguna, Tenerife, Spain
[3] Clarendon Laboratory, University of Oxford, Oxford, UK

E-mail: kaminsky@chem.washington.edu

Received 16 September 2009, in final form 2 January 2010
Published 15 February 2010
Online at stacks.iop.org/JPhysCM/22/095902

Abstract
The anomalous birefringence and circular differential reflection of $NH_4H_2PO_4$ (point group $\bar{4}2m$), cut on the optic axis, have been found to cause an additional signal in measurements of the optical rotation employing polarized light technology, with the sample between crossed and slightly modulated linear polarizers (tilting high accuracy universal polarimetry). The azimuthal rotation of the linearly polarized light, up to 100 times larger than expected, is described in terms of a circularly polarized light mode along the optic axis of varying amplitude. Experimental evidence leading to our conclusion is given and a qualitative model for the effect is presented.

(Some figures in this article are in colour only in the electronic version)

Dedicated to Professor Siegfried Haussühl.

1. Introduction

The state of polarization of light passing through a material may change depending on the symmetry of the medium [1]. The known mechanisms introducing those changes include natural and induced linear refraction plus dichroism and reflection, natural and induced optical rotation (OR), natural or induced circular dichroism (CD), as well as the Raman effect, Cotton Mouton effect, natural and induced Faraday effect, nonlinear optics (SHG), and certain aspects of negative refractive indices [2]. Ferroic media may drastically enhance these interactions [3] not to forget liquid crystals[5] in which these effects are of immense technical and commercial importance.

It is often observed that the chiroptical properties interfere with linear properties and in such cases special techniques are needed to determine the chiroptical strength of a medium. In the past, such techniques have successfully been applied to measure, for example, the optical rotation of crystals where the symmetry is compatible with the existence of chiroptical properties [5]. In particular, the optical rotation strength of $NH_4H_2PO_4$ (ADP) is well understood [6], and its linear refractive indices are known to 5 figures of decimals [7]. In addition, the second harmonic generation (SHG) tensor is established [8] and therefore one should be able to predict the polarization signature of this material for all possible directions of incident light. The optical rotation in tetragonal $NH_4H_2PO_4$ is governed by a second-rank axial tensor. The point group

[4] Author to whom any correspondence should be addressed.
[5] Some of the recent discoveries within the vast field of nematic and cholesteric liquid crystals are listed here, specifically ferroelectric and photoferroelectric liquid crystals [4].

of ADP [9] is $\bar{4}2m$ and the *c*-axis coincides with the optic axis (oa) where light passes through the crystal without the effect of linear birefringence. ADP is birefringent in all other directions, with optical rotation being absent only in the {110} planes (note, that ADP is an optically active, non-enantiomorphic, non-chiral compound [10]).

The measurement of optical rotation in linearly birefringent crystals involves polarimetric methods[6] where incoming and analyzing polarizations are modeled concomitantly with changes of the birefringence of the sample. Such birefringence changes can be induced by varying the temperature, the wavelength, or the direction along which light passes through the material. The latter has been successfully applied to separate optical rotation (a result of circular birefringence) from the much larger effect of linear birefringence via the tilter method [12], where in addition to the so called 'HAUP' set-up [13], the sample is successively rotated about an axis **t** perpendicular to a laser beam and the linear birefringence and optical rotation are derived for each rotation angle.

In applying this technique to a plane-parallel polished plate of optical quality prepared from an ADP crystal, a specific behavior for optical rotation was expected in accordance with numerous other experiments on birefringent crystals and the known experimental properties of ADP [5]. It was therefore surprising to find, that for the special case of a sample that was nearly perfectly cut normal to its four-fold symmetry axis parallel to the oa, a signal was detected that was up to 100 times larger than expected by calculation from the known tensorial properties. The question then arises as to whether this discrepancy could arise from multiple reflections inside the sample, from other imperfections of the device or from the sample itself.

There have been attempts to include multiple reflection in the treatment of OR in birefringent media, which have resulted only in a modulation of the OR reading within the range of a few per cent [14]. The effect of a wedge-shaped sample has been studied as well, showing a decrease of the measured chiroptical values [15].

Below, we outline the experiments that we have carried out, together with a qualitative model to explain our observation[7]. We believe that under certain conditions, circular differential reflection (CDR) [17] on the ADP surface initiates the additional signal which adds to optical rotation with an up to two orders of magnitude larger contribution. We believe that CDR causes a circularly polarized light mode[8] propagating along the optic axis which interferes with the transmitted light. To the best of our knowledge, this mode, which we call a 'surface induced reflective circularly polarized mode, *SIRCPM*' has not been described before.

It is important to understand how *SIRCPM* may affect the outcome of chiroptical measurements, the results of which are otherwise corrupted and therefore difficult to compare with model calculations. Wrong conclusions may otherwise follow affecting our attempts to understand and predict the optical features of crystals.

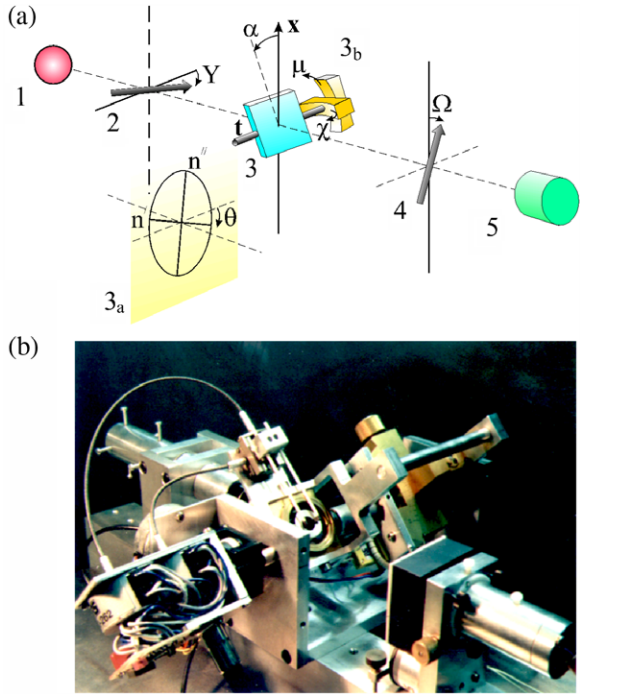

Figure 1. (a) Schematic representation of the tilter device. 1: light source (laser, 670 nm), 2: polarizer (Nicol prism), 3: tilting stage, 3_a: definition of the eigen-ray direction angle θ, 3_b goniometer to adjust the sample orientation, 4: analyzer (Nicol prism), 5: photodiode and preamplifier electronics. (b) photograph of the device. Reproduced with permission from [5]. Copyright 2000 IOP Publishing.

2. Experimental details

2.1. The tilter method

The tilter device [12] (figure 1) represents a modified HAUP set-up and is used to measure chiroptical signals such as optical rotation in the presence of the obscuring effect of linear birefringence and takes into account contributions from small but unavoidable misalignments of the sample and shortcomings of the optical components.

HAUP represents a variant of Mueller–Stokes measurements (MS) which sandwiches a sample between two linearly polarizing modulators [18]. While for MS the modulation of incident and analyzing sections includes many different states of polarization, HAUP only employs linear polarizing components and limits the modulation range to a few degrees which in turn requires the optical eigenmodes of the sample to be well aligned with the incident polarization. The disadvantage of restricted freedom in sample orientation is outbalanced by a much larger sensitivity to OR than general MS.

The resultant output of a HAUP scan is partitioned into a signal related to chiroptical effects, another related to the geometrical alignment of the sample and a third to the phase factor

$$\delta = 2\pi L[n_o - n(\alpha)]/\lambda \qquad (1)$$

[6] Other polarimetric techniques currently used to mainly measure linear birefringence are described here [11].

[7] The additional signal was first mentioned by us during measurements of the optical rotation of pentaerythritol [16].

[8] The term 'circular polarized light' describes a state of light polarization in which the electric field of the light wave rotates about the wave propagation direction. This is mathematically described by two orthogonal linearly polarized waves along the same direction that are out of phase by a quarter wave length.

L denotes the optical path length, n_o the ordinary refractive index in ADP for an eigenmode along the tilt axis, α is the tilt angle measured from the optic axis, λ is the wavelength of the incident light, and $n(\alpha)$ is the refractive index for the eigenmode perpendicular to the tilt axis and the wave propagation direction with wavevector $\boldsymbol{k}$.

As a rule of thumb, the signal-to-noise ratio of a chiroptical contribution to a measurement is optimized if the range of modulation is close to the expected effect. For HAUP, the contribution of OR to the change in detected light intensities for modulations of around 1° is estimated by the expression $\varphi(\boldsymbol{k})\sin(\delta)/\delta$, where $\varphi(\boldsymbol{k})$ is the OR along the wavevector (see equation (18) in appendix A). The OR component perpendicular to the oa in ADP is thus found to account for a few per cent of the measured intensity variations introduced by the polarizer and analyzer modulations (see also equation (6), vide infra).

The normalized intensity I/I_o of the light of amplitude E passing through the polarizer, sample and analyzer, is written approximately as a bi-quadratic polynomial that is normalized to the amplitude of polarizer angles Y^2 and Ω^2 (appendix B):

$$I/I_0 = EE^* = a_0 + a_1 Y + a_2\Omega + a_3\Omega Y + \Omega^2 + Y^2, \quad (2)$$

where Y and Ω modulations are considered to be small (less than 2°). The coefficients a_i are expressed as shown below, with L: sample thickness, ρ optical rotatory power, calibration error $\Delta = Y + 90 - \Omega$, extinction offset angle θ in the plane perpendicular to the wavevector inside the sample, and small residual parasitic ellipticities p and q of the polarizing components.

$$a_1 = 2\left(-\frac{\rho L}{\delta} + p\right)\sin\delta + 2\Delta Y - 2\theta(1-\cos\delta), \quad (3)$$

$$a_2 = -2\left(\frac{\rho L}{\delta} + q\right)\sin\delta + 2\Delta Y\cos\delta + 2\theta(1-\cos\delta), \quad (4)$$

$$a_3 = 2\cos\delta. \quad (5)$$

The chiroptical contribution is obtained from $-(a_1 + a_2)$, the orientation-related signals are derived from $(a_2 - a_1)$, and the phase factor δ is obtained from a_3.

2.2. Sample preparation

Samples of optical quality were cut from a large single crystal grown from aqueous solution and then cut with a wet-wire saw and oriented as well as shaped with sapphire powder and isopropanol as grinding fluid on a glass substrate (figure 2(c)) [19]. The orientation of the sample was established via conoscopic imaging with a polarizing light microscope. The oriented and plane-parallel samples were polished with polishing paper placed on a glass plate and slight amounts of humidity introduced by exhalation resulting in clear, inclusion free, glass-like plates of 1 cm^2 cross-section and of thickness between 0.2 and 2 mm.

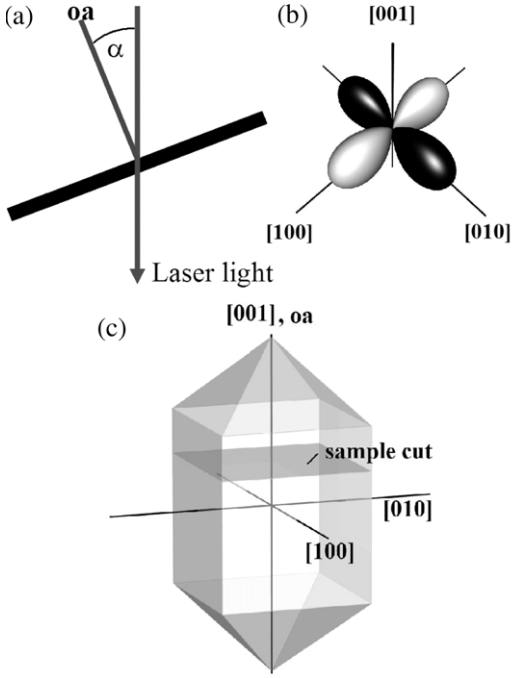

Figure 2. (a) Schematic of the measurement geometry. The ADP sample is cut on the optic axis (oa) and tilted by angle α to introduce birefringence. Strong anomalous signals were observed when the incident polarization is along ⟨100⟩, but no additional signal and no OR is observed for polarizations along ⟨110⟩. (b) The representation surface of OR and amplitude A from equation (8). A change of sign is denoted by lighter versus darker colored lobes. (c) Crystal morphology and sample cut; image prepared with computer program WinXmorph [17].

2.3. First experimental results

With an ADP sample cut normal to the optic axis as shown in figures 2(a) and (c), the value of δ increases with the angle between the laser beam and the optic axis. As a result, the $\cos(\delta)$ signal (parameter $a_3/2$) oscillates with δ. The chiroptical signal, derived from $-(a_1 + a_2)/4$, should show a $\varphi(\alpha)\sin(\delta)/\delta$ dependency (appendix A). The parasitic contribution $\sin\delta(q - p)/4$, although not negligible, is still small. Taking into account the tensorial character of the optical rotation, the corresponding intrinsic rotation angle $\varphi_o(\alpha)$ increases with tilt angle α. The expected signal φ_{OR} for ADP, when cut on the oa, then follows, to a good approximation, for tilt angles below 20° (see appendix C):

$$\varphi_{OR} = c'\sin(c''\alpha^2), \qquad c' = 0.05°, \qquad c'' = \text{constant value}. \quad (6)$$

This expression, however, serves only to estimate the signal strength due to OR. The analysis of the raw intensity readings is made with an exact treatment of birefringence and tensorial character of OR in ADP.

Separating parameters a_1–a_3 into their different contributions allowed us to study the dependence in equation (6) far from the effects of misalignments and parasitic ellipticities. However, the observed behavior consisted of a large contribution to the rotatory signal (figure 3) which was previously

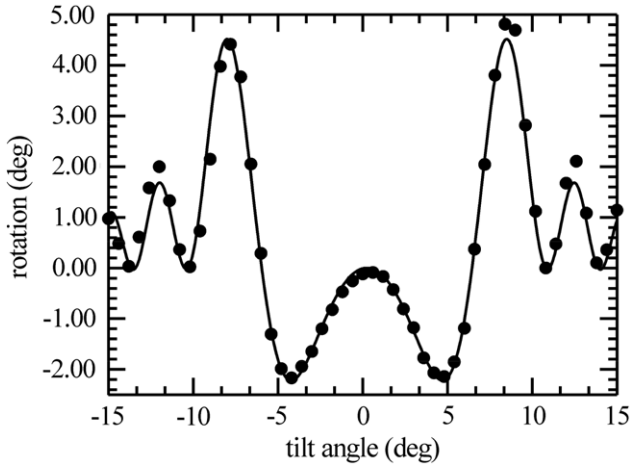

Figure 3. A large signal overlays the expected response. Dots: experimental reading of azimuthal rotation, solid line: equation (5) with fitted amplitude A. The contribution due to optical rotation oscillates within $\pm 0.05°$. The additional signal can reach 5° in ADP, which is 100 times larger than OR, but which varies strongly between samples. Sample thickness 1.32 mm, wavelength 670 nm, Anomalous birefringence was observed along the optical axis with a phase factor $\delta_o = 0.7(1)$, vide infra, figure 6.

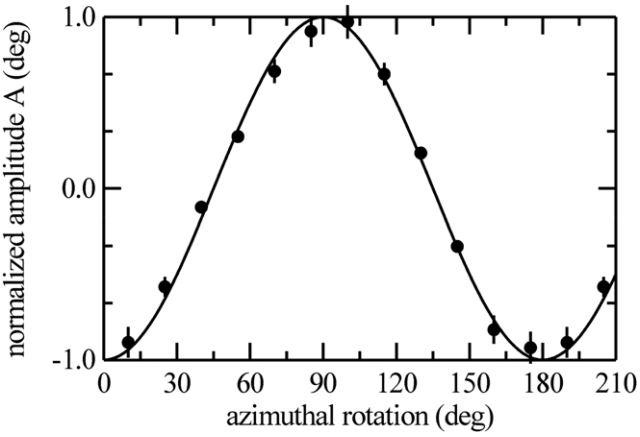

Figure 4. Dependence of amplitude A (normalized) from equation (5) on rotation of the sample about the oa. Two measurements at azimuthal angles σ and $\sigma + 180°$ were averaged. The azimuthal rotation is largest for light polarized along either the a-axis or b-axis[9] . This behavior was observed in all samples, regardless of the maximum observed amplitude A from equation (5) (first 2 points repeated above 180° for clarity). The anomalous phase factor for the data plotted here was about a $\delta_o = 0.1$; see also figure 6.

described by the *empirical* expression [16]

$$\varphi = A\frac{\pi}{2}\frac{\delta}{\pi^2 - \delta^2}\sin^2\left(\frac{\delta - \pi}{2}\right), \qquad (7)$$

where A is a constant amplitude which could not possibly be related to parasitic ellipticities p or q.

To complicate matters, the signal strength of this contribution was found to vary strongly when probing different

[9] We expect to carry out x-ray anomalous scattering experiments in due course to ascertain the absolute structure of our crystal and thus determine which of these two axes applies here.

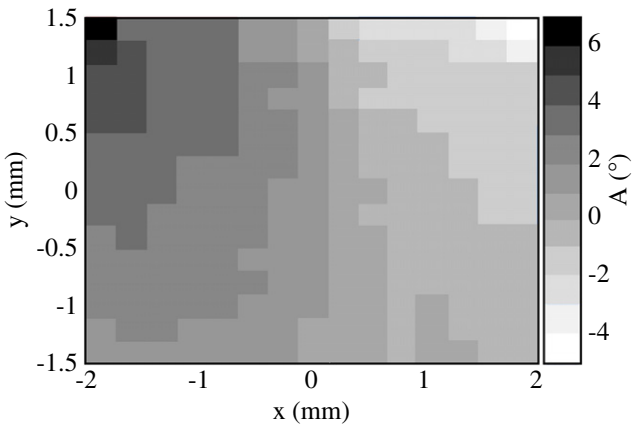

Figure 5. The variation of amplitude A, equation (5), across a sample exhibiting anomalous birefringence along the optic axis. Thickness 1.32 mm, probing wavelength 670 nm.

sample areas or samples. Several tests were performed to elucidate the origin of these confusing observations. The signal was found to depend on the sample preparation, but could not be modeled by inserting an absorption filter after the sample intended to block any second harmonics of the incident laser light. Covering the surfaces with cover slides and oil as immersion fluid was of no significant effect. Most strikingly, when the sample was rotated azimuthally, so that the incident linear polarization would point into different directions in the (001) plane perpendicular to the optic axis, the parameter A followed that for optical rotation, i.e. it vanished for polarizations along ⟨110⟩ and was largest along [100] and of opposite sign along [010] (figures 4, 2(b)).

The irregular dependence of amplitude A of the additional signal from equation (7) on sample preparation was studied in detail taking full tilt scan topographs. A single tilt scan gives information on the three-dimensional orientation of the sample (offsets χ and β_o, see equation (24), appendix B) For a given birefringence of the sample of thickness L, the optical rotatory power, $\rho_{22} = -\rho_{11}$ in ADP, the amplitude of the additional signal A, and concomitant with the offset angle μ, the offset between polarizer and analyzer. Figure 5 shows the color-coded distribution of amplitude A across one of our samples which showed signs of twinning.

Most importantly, the signal was found to be correlated with a small anomalous birefringence with a phase shift up to $\delta_o = 0.7$, causing a small splitting of the optic axis into two axes. The direction of the splitting was along ⟨110⟩ (figure 6, color-coded images in conoscopic geometry employing the Milliview technique [20]). The sample thickness was not found to be important, although the samples needed to be oriented precisely on the optic axis. We also carefully verified that the direction of the axis split was not correlated to the sign of the effect.

3. Discussion

3.1. Numerical simulation of a sample cut on the optic axis

To find an explanation for these findings, which did not arise from errors in the set-up, as is evident by the observed sign

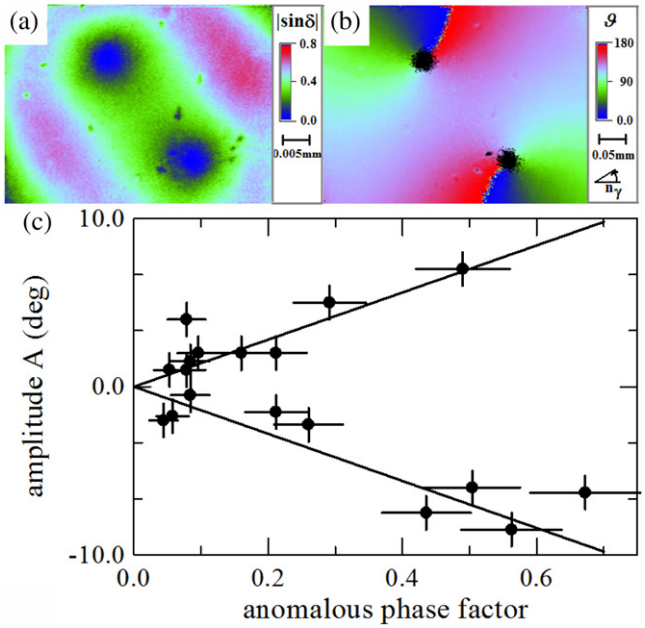

Figure 6. The impact of anomalous birefringence along the optic axis. The splitting of the optic axis (10×—objective, wavelength 550 nm) is in directions ⟨110⟩. (a) Color-coded representation of $|\sin\delta|$. (b) Color-coded extinction angle ϑ of the anomalous birefringence, (c) correlation between A and anomalous birefringence δ_o, which was derived from the calibrated and squared split distance of the optic axis (appendix E, equation (19)). The split direction had no effect on our measurements. Amplitude A was derived from tilt scans similar to those in figure 3 at the same locations where the axis splitting was observed.

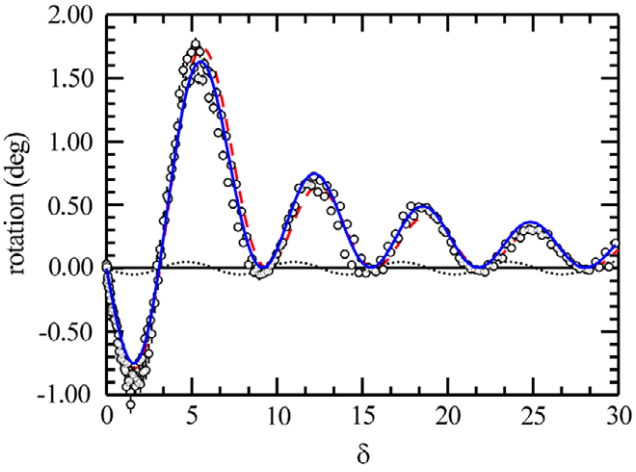

Figure 7. Measured data (open circles) of azimuthal rotation versus phase factor δ and numerical simulation (solid line). The dashed line through the data represents equation (5). The oscillation (dotted line) with small amplitude represents the expected contribution by OR following equation (6). The amplitude A which is the same for the numerical and analytical representations were obtained from a best least-squares fit to the data.

changes under rotation of the sample, we tried a simulation of these measurements via Jones matrices [21] and started by considering the sample to be composed of infinitesimally thin slices.

The optical features of such thin slices may be represented by the products of Jones matrices for infinitesimal circular dichroism (cdr), and linear birefringence, both scaled down to the thickness of a slice. A more or less *accidentally* found expression for a linearly varying cdr along the optical path, $M_{\rm cdr}$, was tried to reproduce the measurement. The iteration starts with Jones vector $J_1 = (E_o, 0)$ representing linearly polarized light. Birefringence is introduced via the phase factor δ:

$$M_{\rm cdr} = \begin{bmatrix} 1 & ip \\ -ip & 1 \end{bmatrix}; \qquad p = A\left(1 - \frac{2k}{m}\right) \tag{8}$$

$$J_{k+1} = \begin{bmatrix} 1 - \frac{i\delta}{2m} & 0 \\ 0 & 1 + \frac{i\delta}{2m} \end{bmatrix} M_{\rm cdr} J_k; \qquad k = 1 \cdots m. \tag{9}$$

Numerical iteration gives a new Jones vector:

$$J_m = (Ex, Ey) = J_m = (E_x, E_y) = E_o(x e^{-id_x}, y e^{-id_y}). \tag{10}$$

With a phase difference of $d = (d_y - d_x)$, the azimuthal rotation is found from the finally resulting Jones vector as [1]

$$2\varphi = \tan^{-1}[2xy\cos(d_x - d_y)/(x^2 - y^2)], \tag{11}$$

and to our surprise, the numerically found dependence, figure 7 gives a good approximation to that of equation (7) which describes the observed signal. Note that the empirical result from equation (7) and that of the numerical procedure are almost indistinguishable. This result, however, was even more confusing because ADP does not absorb light at the probing wave length nor is a varying CD physically meaningful within the understood concepts of optics as described in literature. Moreover, this result does not explain the role of anomalous birefringence which seems to be necessary for this effect to occur.

3.2. Qualitative model for large signal

The meaning of $M_{\rm cdr}$, which is of a circular dichroism type Jones matrix, but with varying component, is to create a circularly polarized light mode along the oa in the first half of the sample and then let it disappear smoothly towards the end of the sample with the amplitude varying parabolically.

This does not imply that ADP is circular dichroic. The principle behind a procedure like the one here employing $M_{\rm cdr}$ is not different to that used to treat optical rotation. The physical interpretation for OA, for example is based on circular birefringence, which can be simulated by a rotation matrix, because the sum of left and right circularly polarized modes of equal amplitudes, but different velocities, into which a linearly polarized wave splits when entering an optically rotatory medium, results in a rotation of the linear polarization. Attributing a rotation of the polarization to the medium as in appendix A, equation (13) simplifies the mathematical description.

Here, we demonstrate how the effective light modes along the oa are caused by multiple circular differential reflections, the effect of which is simulated by a creator/annihilator matrix $M_{\rm cdr}$, equation (8).

ADP is optically active for any angle of light incidence other than within {110} planes. A linearly polarized wave

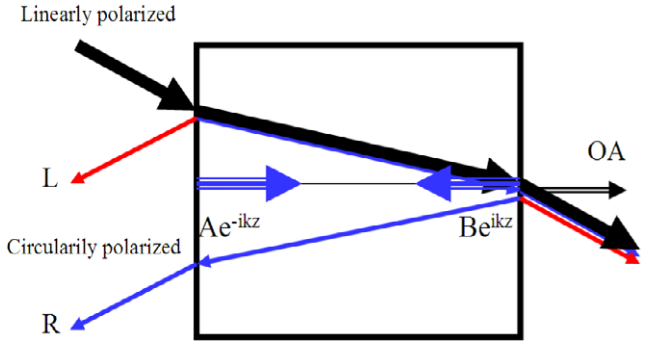

Figure 8. Circular differential reflection on a tilted ADP plate. R(L) denote right(left) circularly polarized light. oa: direction of the optic axis. Fat arrows: incident linearly polarized light. Striped arrows: net circularly polarized light traveling along the optic axis. The reflections of linearly polarized light are not shown for clarity.

can be thought of being composed of two circularly polarized waves (cpw) which will be reflected by different amounts in the presence of optical rotation. This causes a net circular polarization inside the crystal in addition to the transmitted linearly polarized wave. The strength of the CDR effect was estimated from the theoretical treatment by Meteva and Lalov [17]. In interpreting their equations, the CDR is found to be proportional to $\gamma_{11}\varepsilon^3/(\varepsilon_o^2 - \varepsilon_e^2)$, a few per cent in ADP equivalent to possible azimuthal rotations of several degrees[10], where γ_{11} is related to the optical rotatory power, and ε, ε_o, and ε_ε are the dielectric constants at optical frequencies along the incident polarization direction, and along the ordinary, and the extraordinary refractive indices, respectively.

The sample exit face causes CDR as well, but produces reflected and transmitted circular polarizations of opposite hands compared with the entrance face. The transmitted cpw from both surface reflections will cancel out behind the sample in the absence of linear birefringence. The resulting waves and states of polarization (neglecting secondary reflections and linearly polarized reflections) are depicted in figure 8.

Two cdr waves propagate inside the sample, both of the same hand, but traveling in opposite directions. Only those circular polarizations traveling along the optic axis remain unaffected by linear birefringence in a uniaxial crystal like ADP. The waves, however, cannot interfere, because the electric field vectors do not rotate 'synchronously': they rotate in opposite directions. Overlap at any time and position of the waves is minimal.

A small anomalous birefringence along the oa induces a phase shift δ_o between the components of the circularly polarized wave (cpw) inside the sample, seen in projection on the oa. This results in a reduction in the amplitude of the cpw and creates a second circularly polarized wave of opposite hand proportional to $\sin(\delta_o)$ (see appendix D for details). The direction of the anomalous birefringence seems not to be relevant here, whereas it was found to be essential for the creation of anomalous circular extinction, ACE, and anomalous azimuthal rotation, AAR, described by us earlier for dyed crystals showing OR signatures even though the host crystals were centrosymmetric [22].

The wave created by anomalous birefringence is now of opposite hand and thus rotates with the wave returning from the exit face and vice versa. Only the projections on the oa of the transmitted and returning cpw interfere inside the crystal with the projections of the waves created by anomalous birefringence. Similarly, the anomalous birefringence creates a wave of opposite hand out of the returning wave and interference is possible again along the oa. Outside the sample all circularly polarized waves will mainly cancel out. Since the waves created by anomalous birefringence start at zero amplitude on the sample surfaces, no interference wave $C(z)$ is possible on these boundaries.

The problem is symmetric with respect to the intersection in the middle of the sample. At the surfaces (0) and (a) we have no interference as pointed out above. Let $\mathbf{k} \parallel z$ be the wavevector along the **oa**, $A(z)$ and $B(z)$ the amplitudes of cpw due to reflection and anomalous birefringence, then the interference wave results from

$$C(z) = A(z)\mathrm{e}^{-\mathrm{i}ka} + B(z)\mathrm{e}^{\mathrm{i}ka}$$

$$\text{at surface } z = 0: \qquad A(0) + B(0) = 0.$$

Because of cpw being generated out of light along the optic axis with unknown circular polarized amplitude $E(z)$ in proportion to $z\delta_o/a$ (appendix D) we have to assume that $A(z) = z\delta_o E(z)/a$ which forces $A(0) = 0$ and also $B(0) = 0$. The sign of δ_o should not matter, and indeed, we observe the same sign of amplitude A for different optic axis splitting directions. Further we need to consider:

$$\text{at surface } z = a: \qquad A(a)\mathrm{e}^{-\mathrm{i}ka} + B(a)\mathrm{e}^{\mathrm{i}ka} = 0.$$

We are not at liberty to change k to extinguish the exponentials, however, when assuming that $E(z)$ is proportionally to $(a–z)$ this boundary condition is satisfied.

The simplest non-trivial solution that satisfies the system of equations and boundary conditions for all values of z is then achieved with the 'Ansatz' (figure 9):

$$A(z) = B(z) \propto \delta_o z(a - z)/a, \qquad 0 < z < a. \qquad (12)$$

This is consistent with parameter p in the Jones matrix M_{cdr} from equation (8) discussed above in the numerical simulation which is found to produce cpw with parabolically varying amplitudes, figure 10. The integral of p: $\int_0^k A(1 - \frac{2k}{m})\,\mathrm{d}k = A(k - \frac{1}{m}k^2) \underset{k=z,m=a}{\longrightarrow} \frac{A}{a}z(a-z)$ is indeed of the same form as equation (12). Amplitude A in equation (7) is thus in proportion to anomalous birefringence along the optic axis, described by phase factor δ_o.

The physical meaning of this is that the projection along the oa of the circularly polarized waves interfere more when further away from the surfaces, whereas at shorter distances to the surfaces the amplitudes of all interfering waves need to

[10] In [17], the components γ_{11} and γ_{22} of the optical rotation tensor were assumed to be of equal size and sign. For ADP γ_{11} is of opposite sign of γ_{22} and circular polarization caused by reflection changes sign when the sample is rotated around the optic axis by 90°.

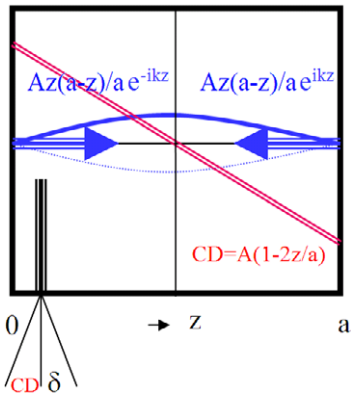

Figure 9. Qualitative model for *SIRCPM*. Striped arrows: two circularly polarized waves travel towards each other and produce additional cpw of opposite hand in the presence of anomalous birefringence. The interference of the waves is represented by a linearly varying CD related matrix component (doubled line). The final interaction with birefringence of the crystal along the wavevector of the incident wave is treated via iteratively multiplying the matrices of the birefringence effects and varying CD of a thin slice.

reach smoothly the boundary condition of vanishing amplitude (figure 9). We abbreviate the name of this mode as *SIRCPM*, a surface induced reflective circularly polarized mode.

If the waves after the sample (see appendix D, equation (30)) do not perfectly cancel out in the presence of normal and anomalous birefringence as well as varying surface qualities any remaining circular polarization is interpreted by HAUP as circular dichroism and this adds to the orientation angle μ. A weak correlation between μ and A was indeed found (see also equation (24) in appendix B which describes how the orientation of the sample affects the experiment).

For incident light propagating along the optic axis *SIRCPM* cancels out. Only if waves along ordinary birefringent directions of the crystal interfere with a projection from the modes along the oa is their presence noticed. The projection of *SIRCPM* on the linearly polarized wave running through the crystal at an angle towards the sample normal vector becomes less favorable at steeper incident angles; however, the projection on the optically active directions will increase to compensate for it, qualitatively explaining why amplitude A in equation (7) is constant over the range of tilt angles in the experiment.

Finally we need to ask if the waves along the oa actually exist. We may answer this first by considering that the laser-illuminated region on the sample is about 50 μm in diameter in our set-up. At a sample thickness above 1 mm and tilt angles of up to 35° it seems unlikely for the incident and returning waves to overlap unless they follow the same path. The only distinguished direction that is tilt angle independent is the one along the optic axis. The energy required to form *SIRCPM* may be understood from circularly polarized Huygens elementary waves from which the interference modes along the optic axis form. Unfortunately, the intensity of any remaining light along the oa outside the sample is very small and may be difficult to detect for an independent proof of our model.

4. Conclusion

We have showed how circular differential reflection can cause an additional signal to measurements of optical rotation employing HAUP when a sample is probed with incident light close to an optic axis. The additional signal requires anomalous birefringence of the sample, without which nothing is observed. The effect is described by a circularly polarized light mode along the optic axis of varying amplitude.

Further work is under way to test our model on crystals of different symmetry, compositions, and the impact of electric fields to induce birefringence, and to complete and refine the theoretical treatment. It will be tested further if this effect can be used to measure optical rotation in uniaxial crystals when induced via an electric field along the c axis which can induce a splitting of the optic axis (see for example [20]) or to measure the electro-optic effect when the optical rotation is known.

Acknowledgments

We are grateful for financial support to the Engineering and Physical Sciences Research Council (EPSRC, UK), the Petroleum Research Foundation (PRF, USA), the NSF-STC Program under Agreement No. DMR-0120967, the Royalty Research Foundation of the University of Washington, Seattle (RRF, USA), the Canary Islands Government (Project No. PI2001/093), and the FPU (AP2000-2139) research grant from the Education, Culture and Sports Ministry of Spain.

Appendix A. Jones formalism for optical rotation and birefringence

Complex optical properties can be represented as the product of individual operators for N successive infinitesimal layers of the sample. Consider the azimuthal rotation φ due to OR after

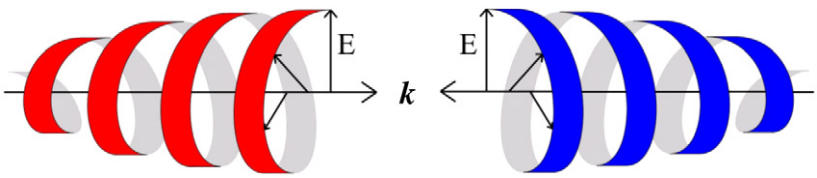

Figure 10. Parabolically varying amplitude of circularly polarized waves along the optic axis as a result of circular differential reflection and anomalous birefringence. The electric fields E of interfering waves rotate with the same sense in the plane normal to wavevector **k** and remain at a constant phase towards each other.

passing through a crystal, with δ, the phase factor. The Jones matrix J_{LB} for linear birefringence (LB), is given below. The accuracy of this is of order N^{-2}. With the expression of the Jones matrices J_{OR} of optical rotation (OR) follows:

$$J_{\mathrm{LB}} = \begin{bmatrix} \mathrm{e}^{\mathrm{i}\delta/2} & 0 \\ 0 & \mathrm{e}^{-\mathrm{i}\delta/2} \end{bmatrix}, \qquad J_{\mathrm{OR}} \approx \begin{bmatrix} 1 & \varphi_{\mathrm{o}} \\ -\varphi_{\mathrm{o}} & 1 \end{bmatrix},$$

$$J_{\mathrm{layer}} = J_{\mathrm{OR}} J_{\mathrm{LB}} \approx \begin{bmatrix} 1 + \mathrm{i}\delta/2N & \varphi_{\mathrm{o}}/N \\ -\varphi_{\mathrm{o}}/N & 1 - \mathrm{i}\delta/2N \end{bmatrix} \tag{13}$$

$$= \left(1, -\mathrm{i}\frac{\delta}{2N}, -\mathrm{i}\frac{\mathrm{i}\varphi_{\mathrm{o}}}{N}\right)\left(\begin{bmatrix} 1 & 0 \\ 0 & 1 \end{bmatrix}, \begin{bmatrix} -1 & 0 \\ 0 & 1 \end{bmatrix}, \begin{bmatrix} 0 & 1 \\ -1 & 0 \end{bmatrix}\right)$$

$$= \left(1, -\frac{\mathrm{i}}{N}T_1, -\frac{\mathrm{i}}{N}T_2\right)(\sigma_0, \sigma_1, \sigma_2) = \sigma_0 - \frac{\mathrm{i}}{N}\mathbf{T}\cdot\boldsymbol{\sigma}.$$

According to Schellman and Jensen [23], the product matrix can be expressed in terms of the Pauli spin matrices or spinors, σ_0, σ_1, and σ_2. The Jones matrix of the whole crystal follows from

$$J_{\mathrm{crystal}} = \left(\sigma_0 - \frac{\mathrm{i}}{N}\mathbf{T}\cdot\boldsymbol{\sigma}\right)^N \approx \mathrm{e}^{-\mathrm{i}\mathbf{T}\cdot\boldsymbol{\sigma}} \tag{14}$$

where $\mathbf{T}$ is a mixed circular and linear phase.

$$\text{With } \mathbf{n} = \frac{\mathbf{T}}{|\mathbf{T}|}; \qquad |\mathbf{T}| \underset{\varphi \ll \delta}{\longrightarrow} \frac{\delta}{2}; \qquad (\mathbf{n}\cdot\boldsymbol{\sigma})^{2j} = \boldsymbol{\sigma}_0,$$
$$j = 1, 2, 3, \ldots \text{ follows} \tag{15}$$

$$J_{\mathrm{crystal}} = \mathrm{e}^{-\mathrm{i}\frac{\delta}{2}\mathbf{n}\cdot\boldsymbol{\sigma}} = \sigma_0 - \mathrm{i}\frac{\delta}{2}\mathbf{n}\cdot\boldsymbol{\sigma} - \frac{1}{2!}\left(\frac{\delta}{2}\mathbf{n}\cdot\boldsymbol{\sigma}\right)^2$$
$$+ \frac{\mathrm{i}}{3!}\left(\frac{\delta}{2}\mathbf{n}\cdot\boldsymbol{\sigma}\right)^3 - \cdots$$
$$= \sigma_0\left[1 - \frac{1}{2!}\left(\frac{\delta}{2}\right)^2 + \frac{1}{4!}\left(\frac{\delta}{2}\right)^4 - \cdots\right]$$
$$- \mathrm{i}\mathbf{n}\cdot\boldsymbol{\sigma}\left[\frac{\delta}{2} - \frac{1}{3!}\left(\frac{\delta}{2}\right)^3 - \cdots\right]$$
$$= \sigma_0 \cos\frac{\delta}{2} - \mathrm{i}\mathbf{n}\cdot\boldsymbol{\sigma}\sin\frac{\delta}{2} = \begin{bmatrix} \mathrm{e}^{\mathrm{i}\frac{\delta}{2}} & \frac{2\varphi_{\mathrm{o}}}{\delta}\sin\frac{\delta}{2} \\ -\frac{2\varphi_{\mathrm{o}}}{\delta}\sin\frac{\delta}{2} & \mathrm{e}^{-\mathrm{i}\frac{\delta}{2}} \end{bmatrix}. \tag{16}$$

It should be noted that this formalism is only successful if the order in which the matrices are multiplied does not matter. In the case of matrices that change during the iterative process, this approach is not applicable, as the order of the matrices is lost when the product of Jones matrices is transformed into a summation $[\exp(-\mathrm{i}\mathbf{T}\cdot\boldsymbol{\sigma})]$.

When we apply J_{crystal} to a 'perfectly' aligned sample, with light that is linearly polarized along the x direction we find:

$$\mathbf{E}' = \mathbf{J}_{\mathrm{crystal}}\begin{pmatrix} 1 \\ 0 \end{pmatrix}\mathbf{E}_0 = \begin{pmatrix} \mathrm{e}^{-\mathrm{i}\frac{\delta}{2}} \\ -\frac{2\varphi_{\mathrm{o}}}{\delta}\sin\frac{\delta}{2} \end{pmatrix}\mathbf{E}_0. \tag{17}$$

Let us define r_x and r_y as the radii of the complex Jones vector components in polar coordinates, and d = phase difference between them, and then

$$\varphi_{\mathrm{observed}} \approx \frac{1}{2}\tan 2\varphi_{\mathrm{observed}} = -\frac{r_x r_y \cos d}{r_x^2 - r_y^2};$$

$$r_x = 1, \quad r_y = -\frac{2\varphi_{\mathrm{o}}}{\delta}\sin\frac{\delta}{2}, \quad d = \frac{\delta}{2},$$

thus

$$\varphi_{\mathrm{observed}} \approx \frac{2\varphi_{\mathrm{o}}}{\delta}\sin\frac{\delta}{2}\cos\frac{\delta}{2} = \varphi_{\mathrm{o}}\frac{\sin\delta}{\delta}. \tag{18}$$

Appendix B. Jones formalism of TILTER equations for non-perfectly aligned samples

Consider a sample placed between two orthogonal polarizers with extinction angle θ. The optical path for the TILTER set-up is represented by a sequence of matrices where A is the light amplitude with rotation matrices for the polarizer (R_Ω), analyzer (R_Y), and sample (R_θ), and parasitic ellipticities of polarizer and analyzer (R_p), (R_q):

$$A = R_q^t R_Y^t \begin{bmatrix} 0 & 0 \\ 0 & 1 \end{bmatrix} R_Y R_q R_\theta^t J R_\theta R_\Omega R_p \begin{bmatrix} 1 \\ 0 \end{bmatrix}, \tag{19}$$

with

$$R_\Omega = \begin{bmatrix} \cos\Omega & -\sin\Omega \\ \sin\Omega & \cos\Omega \end{bmatrix}, \qquad R_Y = \begin{bmatrix} \cos Y & -\sin Y \\ \sin Y & \cos Y \end{bmatrix},$$
$$R_\theta = \begin{bmatrix} \cos\theta_0 & -\sin\theta_0 \\ \sin\theta_0 & \cos\theta_0 \end{bmatrix}, \qquad R_q = \begin{bmatrix} 1 & -\mathrm{i}q \\ \mathrm{i}q & 1 \end{bmatrix},$$
$$R_p = \begin{bmatrix} 1 & -\mathrm{i}p \\ \mathrm{i}p & 1 \end{bmatrix} \tag{20}$$

and

$$J = \begin{bmatrix} \mathrm{e}^{\mathrm{i}\frac{\delta}{2}} & \frac{2\varphi}{\delta}\sin\frac{\delta}{2} \\ -\frac{2\varphi}{\delta}\sin\frac{\delta}{2} & \mathrm{e}^{-\mathrm{i}\frac{\delta}{2}} \end{bmatrix}, \tag{21}$$

representing OR (φ) and linear birefringence (δ).

Further details of the treatment including parasitic ellipticities and the Δy-error (misalignment of polarizer and analyzer) are given elsewhere [10, 24–26]. The product of all matrices can be approximated by a bi-quadratic polynomial that is normalized to the amplitudes of Y^2:

$$I/I_0 = EE^* = a_0 + a_1 Y + a_2\Omega + a_3\Omega Y + a_4\Omega^2 + a_5 Y^2,$$
$$a_1 = 2\left(-\frac{\rho L}{\delta} + p\right)\sin\delta - 2\theta(1 - \cos\delta),$$
$$a_2 = -2\left(\frac{\rho L}{\delta} + q\right)\sin\delta + 2\theta(1 - \cos\delta),$$
$$a_3 = 2\cos\delta. \tag{22}$$

When allowing for a misalignment of the kind $Y = Y' + (\Delta Y)$ and neglecting terms of quadratic order in ΔY, the polynomial transforms into:

$$I/I_0 = a_0' + (a_1 + 2\Delta Y)Y' + (a_2 + 2\Delta Y\cos\delta)\Omega + a_3 Y'\Omega$$
$$+ a_4\Omega^2 + a_5 Y'^2. \tag{23}$$

The first term (a_0') is the overall offset in the intensity measurement.

Furthermore, we need to study the orientation of the sample when it is tilted by angle, α. Inside the sample we observe the angle β. The extinction angle θ is a function of offsets χ_{o}, μ_{o}, and β_{o}, in the sample orientation (see figure B.1).

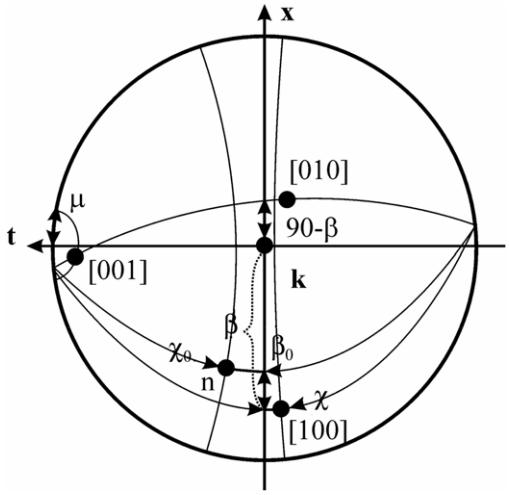

Figure B.1. Stereographic representation of the geometry of a sample with small orientational offsets χ_o, μ_o, and β_o, rotated about tilt axis direction **t** by angle β. The reference coordinates are **t**, wavevector **k**, and the direction **x** perpendicular to $\boldsymbol{t}$ and $\boldsymbol{k}$.

The sample orientation is represented for a small offset χ of the optical eigenmode in the plane given by the plate normal and the tilt axis $\boldsymbol{t}$, and offset μ, which represents a small rotation of eigenmodes around the plate normal (with $\ldots_o$ indicators omitted for clarity):

$$\{u_{ij}\} = \begin{pmatrix} 1 & \mu & 0 \\ -\mu & 1 & \chi \\ 0 & -\chi & 1 \end{pmatrix}.$$

The tilt matrix may be represented by

$$\{v_{kl}\} = \begin{pmatrix} \cos\beta & 0 & \sin\beta \\ 0 & 1 & 0 \\ -\sin\beta & 0 & \cos\beta \end{pmatrix}$$

with polarization tensor a^0_{ij}, $E_i = a_{ij}D_j$, $a^0_{ii} = n_i^{-2}$ and the transformed polarization tensor from $a_{kl} = v_{ki}v_{lj}u_{i\alpha}u_{j\alpha}a^0_{\alpha\beta}$.

From the submatrix representing the plane perpendicular to the wavevector follows:

$$\theta(\beta) \approx \frac{1}{2}\tan 2\theta = \frac{a_{12}}{a_{22}-a_{11}} = \frac{\chi(a^0_{33}-a^0_{22})\sin\beta + \mu(a^0_{22}-a^0_{11})\cos\beta}{a^0_{22}-a^0_{33}\sin^2\beta - a^0_{11}\cos^2\beta}. \quad (24)$$

In a uniaxial sample $a^0_{11} = a^0_{22}$ and μ would be meaningless.

Appendix C. Derivation of $\varphi = c'\sin(c''\alpha^2)$ (equation (6))

We treat the situation where the extraordinary index (n_e) is parallel to the plate normal vector and the tilt axis $\boldsymbol{t}$ is in the plane of the sample. If the birefringence is small (<0.1) the differences in path lengths of the light waves due to double refraction will be negligible. Within the small deviations of the experimental set-up, we can assume the refractive index for incident polarizations to be that of the ordinary index of refraction, n_o. The refractive index for the extraordinary wave is related to n_o and the principal extraordinary index n_e according to [27, 28]:

$$\frac{1}{n'^2} = \frac{\cos^2\beta}{n_e^2} + \frac{\sin^2\beta}{n_o^2}. \quad (25)$$

This can be rewritten as

$$n'^2 = \frac{n_e^2 n_o^2}{n_e^2\cos^2\beta + n_o^2\sin^2\beta} = \frac{n_e^2 n_o^2}{n_e^2(1-\sin^2\beta) + n_o^2\sin^2\beta}$$

and with the assumption of small angles β, and the relation $a^2 - b^2 = (a+b)(a-b)$ as well as $\frac{1}{a+x} \approx \frac{1}{a} - \frac{x}{a^2}$ we find

$$n'^2 = \frac{n_e^2 n_o^2}{n_e^2 + (n_o+n_e)(n_o-n_e)\sin^2\beta} \approx n_o^2\left(1 - \frac{(n_o+n_e)(n_o-n_e)\sin^2\beta}{n_e^2}\right). \quad (26)$$

Thus with $2n = n_o + n_e$ the birefringence $\Delta n = (n_o - n') \approx \frac{1}{2n}(n_o^2 - n'^2)$ can be approximated as

$$\Delta n \approx \frac{n_o^2}{n_e^2}(n_o - n_e)\sin^2\beta. \quad (27)$$

The optical rotation of a uniaxial crystal with point group $\bar{4}2m$ is derived from the only existing rotatory power component $\rho_{11} = -\rho_{22} = \rho$ as

$$\varphi_o = \rho L \sin^2\beta. \quad (28)$$

This leaves us, using the simplification of Snell's law for small tilt angles: $\alpha/\beta = n_o$, and thus with Δn proportional to $\sin^2(\beta)$ or β^2 for the tilt angle range of the shown experiments with $\delta \approx c''\alpha^2$, c'' a constant factor:

$$\varphi_{OR} = \varphi_o\frac{\sin\delta}{\delta} \approx \frac{\rho\lambda n_e^2\sin^2\beta}{2\pi L n_o^2(n_o-n_e)\sin^2\beta}\sin\delta \approx c'\sin(c''\alpha^2). \quad (29)$$

Appendix D. Circularly polarized light passing a slightly birefringent medium

A small anomalous birefringence induces a phase shift δ_o between the components of the circularly polarized wave (cpw) inside the sample following a $\cos(\delta_o)$ dependence. This results in a reduction in the amplitude of the cpw plus a second circularly polarized wave of opposite hand and a phase shift. When following the light path projection along the oa, at a distance z from the surface of a plate of thickness a and anomalous birefringence δ_o, with $f(z) = z\delta_o/2a$ we find for the cpw amplitude, employing Jones formalism:

$$\begin{pmatrix} E_x \\ E_y \end{pmatrix} = \begin{bmatrix} e^{if} & 0 \\ 0 & e^{-if} \end{bmatrix}\frac{1}{\sqrt{2}}\begin{pmatrix} 1 \\ i \end{pmatrix} = \frac{1}{\sqrt{2}}\begin{pmatrix} e^{if} \\ ie^{-if} \end{pmatrix} = \frac{1}{\sqrt{2}}\cos f\begin{pmatrix} 1 \\ i \end{pmatrix} + \frac{1}{\sqrt{2}}\sin f\begin{pmatrix} i \\ 1 \end{pmatrix}. \quad (30)$$

The term in proportion to $\sin(f) \approx z\delta_o/2a$ denotes circularly polarized light of opposite hand to that of the incident wave and is also phase shifted by $\pi/2$.

Appendix E. Anomalous phase factor and optical axis splitting

We are studying the angle between two optic axes, $2V$, introduced by a small difference $\Delta n'$ in the ordinary refractive index along two ortho normal directions perpendicular to the optic axis. Equation (27) can be used to find a relation between $\Delta n'$ and V:

$$\Delta n' \approx \frac{n_o^2}{n_e^2}(n_o - n_e)\sin^2 V.$$

In conoscopic imaging mode with a polarized light microscope, the splitting of the optic axis is measured as a distance d_s between the axes with $\sin(V) \propto d_s$. The anomalous phase factor which is in proportion to $\Delta n'$ is also in proportion to $\sin^2 V$ and, thus, to d_s^2. After deriving the calibration factor c_s from the split distance of a known sample, we find for small values of birefringence $n_o - n_e$:

$$\delta_o = (c_s d_s)^2. \tag{31}$$

Appendix F. Summary of abbreviations and symbols

$[\cdots]$, $\langle\cdots\rangle$	direction, all symmetry-equivalent directions
$(\cdots)$, $\{\cdots\}$	face normal vector, all symmetry-equivalent faces
ADP	$NH_4H_2PO_4$ (ammonium dihydrogen phosphate)
α	tilt angle
A	amplitude of new phenomenon
β	tilt angle inside the sample
β_o	sample orientation offset
CD	circular dichroism
CDR	circular differential reflection
cdr	varying CD related to CDR
cpw	circularly polarized wave
c_s	calibration factor in optic axes split measurements
d, d_x, d_y	phases of complex numbers in polar coordinates
d_s	optic axes split distance in conoscopic images
E, E_x, E_y	electric field vector and Jones vector components
χ	sample orientation offset
δ, δ_o	phase factor due to crystal-, anomalous birefringence
E	electric field strength
HAUP	high accuracy universal polarimetry
$\boldsymbol{J}$	Jones vector
$\boldsymbol{k}$	wavevector (direction of the light wave)
M	Jones matrix
λ	wave length
L	optical path length
μ	sample orientation offset
MS	Mueller–Stokes measurements
$\mathbf{n}$	sample normal vector
n	refractive index perpendicular to n_o and $\mathbf{k}$
n_e	extraordinary refractive index
n_o	ordinary refractive index
oa, **oa**	optic axis and corresponding direction vector
Ω	analyzer modulation angle
OR	optical rotation
φ, φ_o, φ_{OR}	optical rotation angle of a measurement, intrinsic OR, observed OR
r_x, r_y	radii of complex numbers in polar coordinates
ρ	rotatory power
SHG	second harmonic generation
$\boldsymbol{t}$	tilt axis direction
θ, ϑ	extinction angle in HAUP-, in Milliview device
$2V$	optic axes split angle
x, y, z	Cartesian coordinates
Y	polarizer modulation angle

References

[1] Haussühl S 1983 *Kristallphysik* (Weinheim: Physik Verlag, Verlag Chemie)

[2] See as an example, Pendry J B 2000 *Phys. Rev. Lett.* **85** 3966–9

[3] See for example, Kaminsky W 1994 *Phase Transit.* **52** 235–59
Kaminsky W 1997 *Ferroelectrics* **204** 233–46

[4] Langhoff A and Giesselmann F 2002 *J. Chem. Phys.* **117** 2232–7
Details on the electroclinic effect and liquid crystal enhancement of chiral perturbations, Kapernaum N, Walba D M, Korblova E, Zhu C, Jones C and Shen Y 2009 *ChemPhysChem* **10** 890–2
De Fries Materials, Lagerwall S T, Rudquist P and Giesselmann F 2009 *Mol. Cryst. Liq. Cryst.* **510** 148–57
Chiral smectic liquid crystals from non-chiral molecules, Hough L E, Spannuth M, Nakata M, Coleman D A, Jones C D, Dantlgraber G, Tschierske C, Watanabe J, Korblova E, Walba D M, Maclennan J E, Glaser M A and Clark NA 2009 *Science* **532** 452–6
Light scattering in liquid crystals, Loiko V A, Konkolovitch A V and Miskevich A A 2009 *J. Exp. Theor. Phys.* **108** 535–45
Gennes P G D 1977 *Mol. Cryst. Liq. Cryst.* **34** 177–82
Memory applications, Muravsky A, Murauski A, Chigrinov V and Kwok H S 2008 *J. Soc. Inform. Disp.* **16** 927–31
Antonova K T, Dozov I and Martinot-Lagarde P 2004 *J. Mol. Struct.* **704** 329–33
Surface effects in liquid crystals, Gorkunov M and Pikin S 2002 *Eur. Phys. J.* E **9** 27–34

[5] Kaminsky W 2000 *Rep. Prog. Phys.* **63** 1575–640

[6] Stadnicka K, Madej A, Tebbutt I J and Glazer A M 1992 *Acta Crystallogr.* B **48** 16–21

[7] Landolt-Boernstein 1969 *Ferro- and Antiferroelectric Substances* (*New Series* vol 3) (Berlin: Springer)

[8] Craxton R S 1981 *IEEE Quantum Electron.* **17** 1771–82

[9] Kahn A A and Bauer W H 1973 *Acta Crystallogr.* B **29** 2721–6

[10] Claborn K, Isborn C, Kaminsky W and Kahr B 2008 *Angew. Chem. Int. Edn* **47** 2–14

[11] Safrani A and Abdulhalim I 2009 *Opt. Eng.* **48** 053601–10
Giesselmann F and Langhoff A 2002 *ChemPhysChem* **3** 424–32
Ajovalasit A, Barone S and Petrucci G 1998 *J. Strain Anal.* **38** 75–92
Oldenbourg R and Mei G 1995 *J. Microsc. Oxford* **180** 140–7
Glazer A M, Lewis J G and Kaminsky W 1996 *J. R. Soc. Lond.* A **452** 2751–65

[12] Kaminsky W and Glazer A M 1996 *Ferroelectrics* **183** 133–41
Kaminsky W 1996 *Phase Transit.* **59** 121–33

Mucha D, Stadnicka K, Kaminsky W and Glazer A M 1997 *J. Phys.: Condens. Matter* **9** 10829–42
Kim D-Y, Kaminsky W and Glazer A M 2001 *Phase Transit.* **73** 533–63
Kaminsky W, Thomas P A and Glazer A M 2002 *Z. Kristallogr.* **217** 1–7
[13] Kobayashi J and Uesu Y 1983 *J. Appl. Crystallogr.* **16** 204–11
Kobayashi J, Uesu Y and Takehara H 1983 *J. Appl. Crystallogr.* **16** 212–9
[14] Bachheimer J P 1986 *J. Phys. C: Solid State Phys.* **19** 5509–17
Folcia C L, Ortega J and Extebarria J 1999 *J. Phys. D: Appl. Phys.* **32** 2266–77
Simon J, Weber J and Unruh H-G 1997 *J. Phys. D: Appl. Phys.* **30** 676–82
[15] Kaminsky W and Hartmann E 1993 *Z. Phys.* B **90** 47–50
Herreros-Cedres J, Hernandez-Rodrıguez C and Guerrero-Lemus R 2006 *J. Opt. A: Pure Appl. Opt.* **8** 44–8
[16] Claborn K, Kaminsky W, Herreros-Cedres J, Weckert E and Kahr B 2006 *J. Am. Chem. Soc.* **128** 14746–7
[17] Miteva A I and Lalov I J 1993 *J. Phys.: Condens. Matter* **5** 6099–110
[18] Stokes G G 1852 *Trans. Camb. Phil. Soc.* **9** 399–416
[19] Kaminsky W 2005 *J. Appl. Crystallogr.* **38** 566–7
Kaminsky W 2007 *J. Appl. Crystallogr.* **40** 382–5
[20] Kaminsky W, Gunn E, Sours R and Kahr B 2008 *J. Microsc.* **228** 153–64
[21] Jones R C 1941 A new calculus for the treatment of optical systems *J. Opt. Soc. Am.* **31** 488–93
Jones R C 1941 A new calculus for the treatment of optical systems *J. Opt. Soc. Am.* **31** 493–9
Jones R C 1941 A new calculus for the treatment of optical systems *J. Opt. Soc. Am.* **31** 500–3
Jones R C 1942 A new calculus for the treatment of optical systems *J. Opt. Soc. Am.* **32** 486–93
Jones R C 1947 A new calculus for the treatment of optical systems *J. Opt. Soc. Am.* **37** 107–10
Jones R C 1947 A new calculus for the treatment of optical systems *J. Opt. Soc. Am.* **37** 110–12
Jones R C 1948 A new calculus for the treatment of optical systems *J. Opt. Soc. Am.* **38** 671–85
Jones R C 1956 A new calculus for the treatment of optical systems *J. Opt. Soc. Am.* **46** 126–31
[22] Kaminsky W, Geday A M, Herreros-Cedres J and Kahr B 2003 *J. Phys. Chem.* A **107** 2800–7
Kaminsky W, Herreros-Cedres J, Geday M A and Kahr B 2004 *Chirality* **15** 855–61
[23] Schellman J and Jensen H P 1987 *Chem. Rev.* **87** 1359–99
[24] Moxon J R L and Renshaw A R 1990 *J. Phys.: Condens. Matter* **2** 6807–36
[25] Hernandez-Rodriguez C, Gomez-Garrido P and Veintemillas S 2000 *J. Appl. Crystallogr.* **33** 938–46
[26] Kaminsky W 1996 *Phase Transit.* **59** 121–33
[27] Hartshorne N H and Stuart A 1964 *Practical Optical Crystallography* (London: Edward Arnold Publishers)
[28] Nye J F 1985 *Physical Properties of Crystals* 2nd edn (Oxford: Clarendon)